NUCLEAR QUADRUPOLE COUPLING TENSOR OF CH_2Cl_2: COMPARISON OF QUADRUPOLAR AND STRUCTURAL ANGLES IN METHYLENE HALIDES

Z. Kisiel, J. Kosarzewski and L. Pszczółkowski

Institute of Physics, Polish Academy of Sciences
al. Lotników 32/46, 02-668 Warszawa, Poland

(Received April 29, 1997)

Nuclear quadrupole hyperfine structure in $2_{1,2} \leftarrow 3_{0,3}$ and $1_{1,1} \leftarrow 2_{0,2}$ rotational transitions of $CH_2{}^{35}Cl_2$ at 9.2 and 15.9 GHz, respectively, was measured with a newly constructed pulsed supersonic beam, cavity Fourier transform microwave spectrometer. All components of nuclear quadrupole splitting tensors of the chlorine nuclei in inertial and in principal quadrupole axes were determined. It is shown that in methylene halide molecules nuclear quadrupole information leads to a value for $\angle$(XCX) which is systematically larger than $\angle$(XCX) defined by the positions of the nuclei. Some novel features of the spectrometer are also described.

PACS numbers: 33.15.Dj, 33.15.Pw, 33.20.Bx

1. Introduction

The increasing use of molecular beam spectroscopic techniques, which allow high-resolution studies in the sub-Doppler regime, currently provides insight into many hitherto unknown molecular properties. It is now, for example, possible to determine fine details of electron distribution in standard covalent bonds, which are conventionally assumed to be cylindrically symmetric about the axis joining the bound nuclei. Accurate studies of nuclear quadrupole coupling allow measurement of the previously elusive off-diagonal components of the nuclear quadrupole splitting tensor in asymmetric top molecules, so that diagonalization of this tensor is possible, and the orientation of its principal axes can be determined. Nuclear quadrupole splitting constants $\chi_{\alpha\alpha}$ are proportional to the field gradients $\partial^2 V/\partial\alpha^2$. For a quadrupolar nucleus terminal to a cylindrically symmetrical chemical bond the principal quadrupole tensor elements are related, in view of Laplace's equation, by $\chi_{zz} = -(\chi_{xx} + \chi_{yy})$ and $\chi_{xx} = \chi_{yy}$, and the z-axis is collinear with the internuclear bond axis. In practice, the electron density about the z-axis is

slightly deformed as indicated by non-zero values of the quadrupole asymmetry parameter $\eta = (\chi_{xx} - \chi_{yy})/\chi_{zz}$, and the z-axis is not exactly collinear with the bond axis. There is considerable literature on the use of η to characterize such quantities as the amount of π-character of bonds [1], yet little is known about the trends concerning the divergence between bond direction and the direction of the symmetry axis of electron density. Good agreement between directions of the z-axis and the bond axis has often been noted, although, to our knowledge, there has been little discussion of possible systematic differences. One of the reasons was that usually either the quadrupolar or the structural information was less precise than the difference between the two.

Accurate information of this type has recently become available for two members of the methylene halide series, CH_2Br_2 [2] and CH_2I_2 [3]. For CH_2Cl_2 principal nuclear quadrupole splitting constants have been determined in a pioneering study of off-diagonal quadrupole contributions [4] although the attained precision is insufficient for comparison against structural information. Quadrupole splitting constants of chlorine nuclei are much smaller than those of the two heavier halogens and off-diagonal contributions to frequencies of rotational transitions normally do not exceed several tens of kHz, unless a suitable perturbation is present [5, 6]. The use of sub-Doppler spectroscopic methods which, in the microwave region, are characterized by measurement accuracy at the single kHz level, allows precise determination of such effects in the general case. Presently we report the results of measurements of nuclear quadrupole structure in the rotational spectrum of CH_2Cl_2 with a pulsed supersonic beam, cavity Fourier transform microwave (FTMW) spectrometer. Comparison between angular information available from quadrupole constants with structural angles for the methylene halide molecules is made and reveals systematic trends which are discussed. Several novel features of our spectrometer are also described.

2. Experimental details

The measurements were carried out with the newly commissioned, pulsed supersonic nozzle, cavity FTMW spectrometer at the Institute of Physics, Warsaw (Fig. 1). The spectrometer is based on the well established Balle–Flygare design [7] but it embodies several key modifications for ease of use and improved sensitivity.

The spectrometer consists of a 60 cm diameter vacuum chamber which is pumped, through a 40 cm diameter cut-off valve, by a 5000 l s^{-1} oil diffusion pump backed by a 100 m^3 h^{-1} rotary pump, produced by TEPRO, Poland. The vacuum chamber is provided with a hinged door so that the microwave resonator, which is constructed as a self-supporting module, can easily be moved in or out. One mirror of the resonator is linked to a computer controlled translation stage and the resonator can be tuned by monitoring the signal reflected from the resonator with a digital voltmeter. Automatic scanning under computer control is therefore possible. The small L-type coupling aerials in the centers of the mirrors can also be moved from outside the vacuum chamber by means of appropriate mechanical linkages.

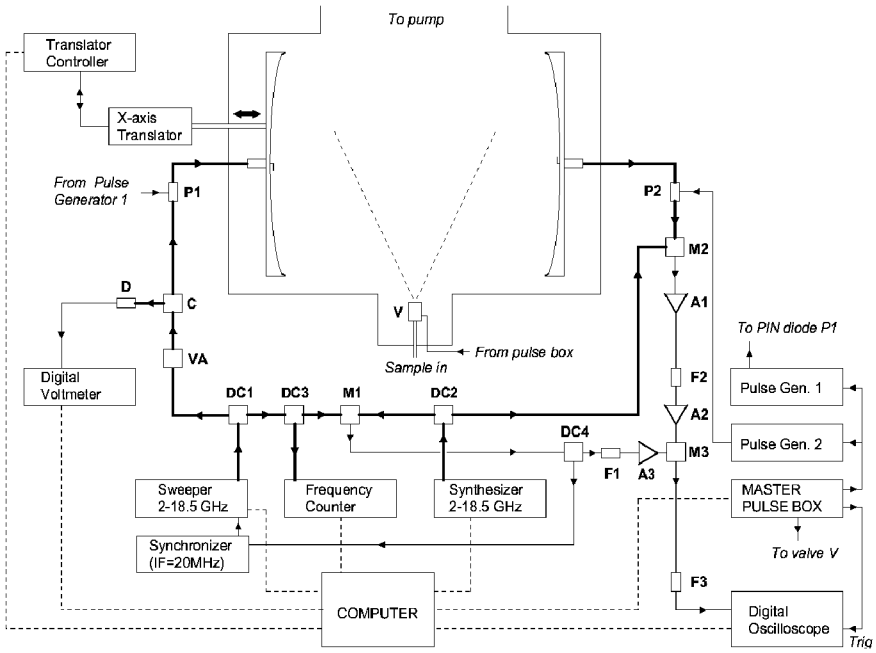

Fig. 1. Schematic diagram of the cavity Fourier transform microwave spectrometer at the Institute of Physics. Full lines denote the path of the microwave signal and, with the exception of the microwave circulator and the coupling aerials, all elements in this path operate over 2–18 GHz. The marked microwave signal processing elements are $P1, P2$ — Narda SP-213DHS80 PIN diodes, $DC1, DC2$ — Narda 4203-10, 10 dB directional couplers, $DC2$ — Narda 4203-6, 6 dB directional coupler, VA — two Narda 4741R 9 dB variable attenuators connected in series, $M1, M2$ — Miteq DB0218LW2 mixers, C — circulator, one of Microwave International F7117-04FFF (2–4 GHz), Teledyne Microwave C-4S63U-50 (4–8 GHz) or C-7S83U-40 (7.6–18 GHz), D — HP-8472B detector. The marked RF signal processing elements are $M3$ — Mini-Circuits ZP-10514 RF-mixer, $A1$ — Miteq AU-4A-0110, 60 dB gain amplifier, $A2$ — Mini-Circuits ZFL-500LN, 25 dB gain amplifier, $A3$ — Miteq AU-3A-0110 amplifier, $DC4$ — Mini-Circuits ZFDC-10-1 10 dB directional coupler, $F1, F2$ — Mini-Circuits BIF21.4 20 MHz band-pass filters, $F3$ — 0.5 MHz low-pass anti-aliasing filter. Dotted lines denote GP-IB connections.

The microwave signal path is constructed entirely from broad band coaxial elements and the diameter of the resonator mirrors was increased to 50 cm so that the low-frequency limit of diminishing performance (Fresnel number of unity) was lowered to 4.5 GHz. The two microwave sources, the HP-8672A synthesizer and the HP-8620C/HP-86290C sweeper are locked together by means of the HP-8709A synchronizer, and provide remotely controlled operation over the whole design 2–18.5 GHz frequency range of the spectrometer.

A flexible data acquisition system was constructed on the basis of an averaging digital oscilloscope (LeCroy 9310A). The only purpose designed electronic

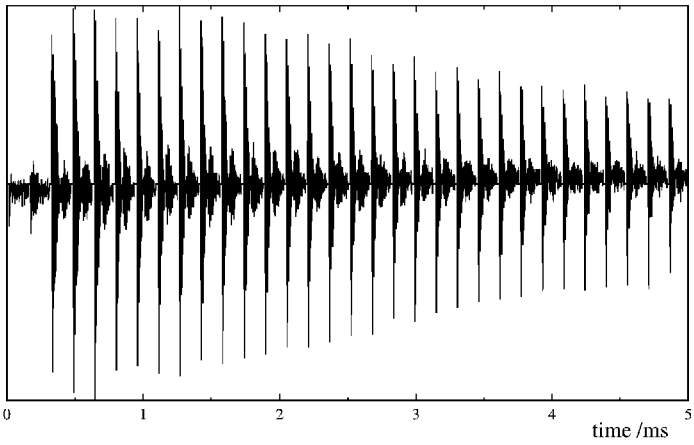

Fig. 2. The averaged 10000 point oscilloscope record obtained by adding wave forms from 100 pulses of Ar gas seeded with CH_2Cl_2. On transition of the molecular beam through the cavity 32 consecutive microwave pulses were applied at excitation frequency of 9277.1203 MHz. The timings were chosen so that signal obtained for the first two microwave pulses illustrates spectrometer response just prior to the arrival of the gas pulse. Spurious transients from the first 15 μs directly following the 200 ns exciting microwave pulse were suppressed for clarity and intensities are in arbitrary units.

module, the "master pulse box", allows appropriate sequencing of up to 99 microwave pulses per single gas pulse. The sample is pulsed into the vacuum chamber through a 0.35 mm orifice in a backing plate attached to a General Valve Corp. Series 9 valve with 0.5 mm output diameter. The small secondary expansion chamber created in this way extends the usable duration of gas expansion to 5 ms, as illustrated in Fig. 2. Wide variation of the number and spacing of the exciting microwave pulses per gas pulse is possible, and typically from 20 to 80 microwave relaxation signals were recorded per single gas pulse. The multipulse time-domain interferogram, of the type shown in Fig. 2, is autonomously averaged within the oscilloscope over as many gas pulses as necessary. The acquired information is transferred to the computer only on completion of the measurement, the individual microwave segments are then coadded, and the result subjected to the fast Fourier transform (FFT) procedure to yield the frequency-domain spectrum. The hardware and signal processing purpose-built software allow for various compromises between resolution and sensitivity, as illustrated in Fig. 3. For example, during analysis of complex hyperfine patterns, the FFT of only the first wave packet of the relaxation signal can be used to simplify the spectrum by eliminating the Doppler doubling. Alternatively, in a spectrum like that in Fig. 3, only the first 65 μs of the relaxation signal could be recorded. This would increase S/N by more than doubling the number of microwave pulses during a single gas pulse, although it would be at the cost of decreasing precision of frequency measurement by a corresponding factor. Various signal processing options such as background subtraction, variable amount of zero filling prior to carrying out the FFT, or alter-

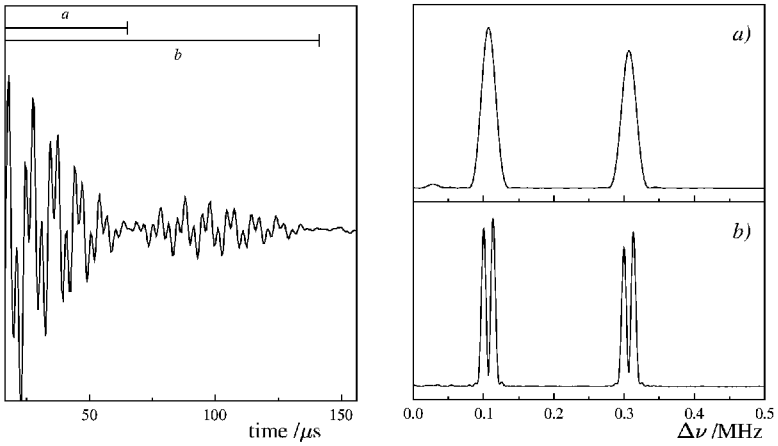

Fig. 3. The 270 point time domain interferogram (a) resulting from coaddition of segments visible in Fig. 2 and its frequency domain spectra obtained by using (b) only the first wave packet and (c) the first two wave packets in the FFT procedure. The intensities are in arbitrary units, the point spacing in the interferogram is 0.5 μs, and the data was zero filled up to 4096 points, so that point spacing in the frequency domain is 0.488 kHz. The two transitions are both to high frequency from the excitation frequency of 9277.1203 MHz, at frequencies of 9277.2273 and 9277.4267 MHz.

ing the apparent relaxation time of the recorded interferogram were also used to aid analysis. The speed of contemporary personal computers allows considerable amounts of zero filling, since with the P120 computer used in the spectrometer FFT of 16384 data points programmed with standard software tools [8] takes less than one second. For this reason the measured line contours no longer have to be subject of insufficient data points in the frequency-domain, which affected earlier work [9]. Although schemes employing multiple microwave pulses for a single gas pulse have been reported previously [10], ours has the advantage of considerably greater flexibility in the choice of acquisition parameters.

The molecular beam was generated by expanding the mixture of *ca.* 2% of CH_2Cl_2 in Ar carrier gas into the high vacuum chamber of the spectrometer, from a backing pressure of 0.7 atm at a rate of 2 Hz. The signal was averaged over several tens to several hundred gas pulses, depending on the intensity of the measured spectroscopic transition. Several of the known techniques for increasing sensitivity, such as the use of a microwave amplifier before the detecting mixer $M2$, or pulsing the sample along the resonator axis, still remain to be explored. Nevertheless current sensitivity was sufficient for observation of the rare isotopic species of a van der Waals dimer, ^{36}Ar...H^{35}Cl, the abundance of which is 0.3% of the parent isotopomer [11].

3. Results

The rotational spectrum of CH_2Cl_2 is allowed by the non-zero μ_b dipole moment component. In the frequency region 2–18 GHz only two ^bP-type rotational

TABLE I

Quantum number assignments, observed (MHz) and observed-calculated (kHz) frequencies for the measured hyperfine splitting components for two rotational transitions of $CH_2{}^{35}Cl_2$.

I' F'	I'' F''	obs.	o-c	I' F'	I'' F''	obs.	o-c
$2,1,2 \leftarrow 3,0,3$				$1,1,1 \leftarrow 2,0,2$			
3 3	3 2	9261.0932	–0.6	3 2	3 1	15897.0883	–0.9
3 2	3 1	9266.1329	0.4	1 2	3 1	15898.0072	0.4
3 4	1 4	9268.6529	0.7	3 2	1 2	15899.6867	–1.4
1 3	1 3	9270.6260	0.8	1 1	1 2	15899.9534	–0.5
3 2	3 2	9272.5198	–1.2	0 1	0 2	15900.5380	0.8
3 3	3 3	9272.6754	–0.2	2 2	0 2	15901.0793	–0.6
3 4	3 3	9275.5390	0.6	3 4	3 5	15906.0996	2.7
3 1	3 0	9275.8646	0.9	3 2	1 3	15908.6488	–1.5
3 4	3 5	9277.2273	1.0	1 2	1 3	15909.5679	–0.1
3 5	3 6	9277.4267	0.7	3 3	1 3	15909.8315	–0.8
1 1	1 2	9278.1896	0.5	3 2	3 2	15911.6543[a]	–0.9
0 2	0 3	9278.5578	0.5	1 1	3 2	15911.9203[a]	–0.7
2 3	2 4	9278.7240	–3.2	2 3	2 4	15912.2743[a]	–1.8
2 4	2 5	9278.7645	–1.7	1 2	3 2	15912.5723	–0.6
2 1	2 1	9278.7774[a]	–1.1	1 1	1 1	15920.5181	–0.7
2 2	2 3	9278.9805	1.1	3 4	3 4	15921.07195	3.7
1 2	1 3	9279.1797	0.6	3 3	3 4	15921.8130	–1.5
1 3	1 4	9280.0681	0.6	1 0	1 1	15921.6358	–2.4
3 3	3 4	9280.1563	1.3	2 3	2 2	15923.4813	0.5
3 4	3 4	9283.0193	1.5	2 1	2 2	15924.0770	–0.2
3 2	3 3	9284.1029	–0.0	1 2	3 3	15924.5597	0.5
1 3	3 3	9286.9540	0.3	3 3	3 3	15924.8232	–0.4
0 2	2 2	9289.4175	–2.3				
2 3	2 3	9289.6509	–1.2				
3 5	3 5	9291.4848	1.4				

[a]Transition assigned measurement error of 4 kHz, the error was otherwise set equal to 2 kHz.

transitions, $2_{1,2} \leftarrow 3_{0,3}$ and $1_{1,1} \leftarrow 2_{0,2}$, are expected to be observable at the low, sub 10 K, rotational temperature of the molecular beam spectrometer. The frequencies of many hyperfine components for both of these transitions were measured and are reported in Table I. For CH_2Cl_2, in which there are two symmetry equivalent chlorine nuclei, the optimum analysis of the hyperfine structure is through

the I, F coupling scheme of nuclear spins with molecular angular momentum [1]. The hyperfine quantum numbers are thus $I = I(\mathrm{Cl}_1) + I(\mathrm{Cl}_2)$, $F = I + J$ and, for P-type transitions, the most intense hyperfine components are $\Delta I = 0$, $\Delta F = -1$. The Hamiltonian matrix was constructed by combining Watson's A-reduced pure rotational Hamiltonian H_r [12] with the splitting Hamiltonian H_q set up using spherical tensor methods [1]. The powerful program suite written by Pickett was used [13]. Graphical display programs were used to identify and select for measurement hyperfine components with the highest contributions from the off-diagonal quadrupole constant χ_{ab}.

TABLE II

The fitted and the derived spectroscopic constants for $CH_2{}^{35}Cl_2$ resulting from analysis of nuclear quadrupole hyperfine splitting structure due to the two chlorine nuclei.

		Fitted[a]			Derived[a]
A	[MHz]	[32002.2900(60)][b]	χ_{bb}	[MHz]	1.8004(12)
B	[MHz]	3320.28126(6)			
C	[MHz]	[3065.22985(66)][b]	χ_{zz}	[MHz]	−75.35(21)
			χ_{xx}	[MHz]	35.41(21)
χ_{aa}	[MHz]	−41.7418(11)	$\chi_{yy} = \chi_{cc}$	[MHz]	39.9414(12)
$\chi_{bb} - \chi_{cc}$	[MHz]	−38.1411(22)			
$\chi_{ab}{}^c$	[MHz]	50.93(23)	$\Theta_{za}{}^c$	[deg]	33.43(5)
			$\angle(\mathrm{CCl}.a)^d$	[deg]	34.11(2)
M_{cc}	[kHz]	1.88(15)			
			η^e		0.060(3)
N_lines		47			
σ_fit	[kHz]	1.28			

[a] The reported uncertainties are standard errors in units of the last quoted digit.
[b] Assumed value, Ref. [14], standard error determined therein is reproduced in brackets. Quartic centrifugal distortion constants from Ref. [14] have also been assumed.
[c] Angle between the principal quadrupole axis z and the principal inertial axis a.
[d] Angle between the CCl bond and the inertial a axis, Ref. [15].
[e] $\eta = (\chi_{xx} - \chi_{yy})/\chi_{zz}$.

The values of spectroscopic constants resulting from fitting the measured transition frequencies are given in Table II. Rotational and centrifugal distortion constants determined in the high-resolution far-infrared (FIR) study of CH_2Cl_2 have been assumed [14]. The deviation of fit is seen to be well within the value of 2 kHz generally assumed for the precision of measurement with the cavity FTMW method. The analysis of FTMW measurements requires more precise information about H_r than is provided by the FIR constants and inclusion of rotational constant B in the fit reduces deviation of fit from 2.28 kHz to 1.28 kHz.

Its fitted value $B = 3320.28126(6)$ MHz is, however, consistent with the FIR value of 3320.28179(63) MHz. The frequency accuracy of FTMW measurements is also sufficient to observe spin-rotation effects. Spin rotation Hamiltonian $H_{\rm sr} = \boldsymbol{M} \cdot \boldsymbol{I}(\mathrm{Cl}_1) + \boldsymbol{M} \cdot \boldsymbol{I}(\mathrm{Cl}_2)$ [16] was added to $H_{\rm r} + H_{\rm q}$, and the transitions measured here were found to determine the M_{cc} component of the spin-rotation tensor, as listed in Table II. Although the experimental values of spin-rotation constants in asymmetric top molecules are still not very well understood, the present value is consistent with the magnitude of several kHz typically determined for the chlorine nucleus [16].

The CH_2Cl_2 molecule is oriented in the inertial axes so that the heaviest nuclei lie in the ab inertial plane, as illustrated in Fig. 4. Thus the only non-zero off-diagonal quadrupole constant is χ_{ab}, although it should be remembered that $\chi_{ab}(\mathrm{Cl}_1) = -\chi_{ab}(\mathrm{Cl}_2)$ [3, 4]. Diagonalization of the quadrupole tensor measured in the inertial axes frame will correspond to rotation through the angle θ_{za} defined by $\tan(2\theta_{za}) = 2\chi_{ab}/(\chi_{aa} - \chi_{bb})$. The derived values for the components of the principal quadrupole tensor and for the rotation angle are also given in Table II.

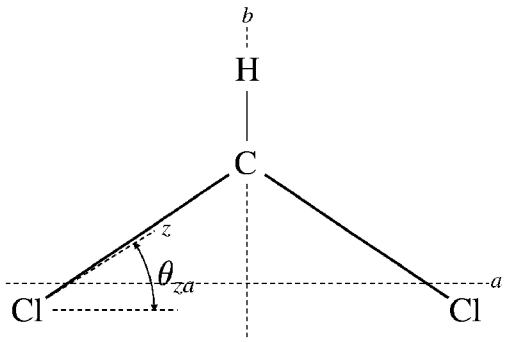

Fig. 4. The orientation of the CH_2Cl_2 molecule in the inertial axes. The difference between the orientation of the quadrupole principal axis z and the axis of the CCl bond was exaggerated although it is in the direction consistent with the experimental result.

The presently determined values of χ_{ab} and of principal quadrupole coupling constants for CH_2Cl_2 compare with $\chi_{ab} = 52(3)$ MHz, $\chi_{zz} = -76(4)$ MHz, and $\chi_{xx} = 36(4)$ MHz determined in [4]. The value $\theta_{za} = 34 \pm 1°$, which was the primary quantity determined in [4], and was one of the first such determinations, is seen to have been quite reliable, since the present more precise value is well within the previous error bounds.

4. Discussion

The present paper completes the data necessary for comparison of angular quadrupole information with structural angles for three lightest quadrupolar methylene halides at accuracies which allow differences to be assessed with significance. The comparison is presented in Table III and it can be seen that the quadrupolar angle θ_{za} is systematically smaller by 0.7–1.1° than the angle between

TABLE III

Comparison of angular information for methylene halides and related molecules derived from nuclear quadrupole analysis with that from the molecular structure.

	$\angle(\mathrm{CX}.a)^a$	Ref.	$\theta_{za}{}^b$	η^c	Ref.
CH_2Cl_2	34.11(2)	[15]	33.42(5)	0.060(3)	This work
CH_2Br_2	33.83(4)	[17]	32.93(4)	0.0417	[2]
CH_2I_2	33.13(7)	[3]^d	32.00(1)	0.0213	[3]

[a] Angle between the CX bond and the inertial a axis, equal to $90^\circ - \angle(\mathrm{XCX})/2$.
[b] Angle between the principal quadrupole axis z and the principal inertial axis a.
[c] $\eta = (\chi_{xx} - \chi_{yy})/\chi_{zz}$.
[d] Revised value obtained from combined results for CH_2I_2 and CD_2I_2, to be published.

the CX bond and the a-axis. There is also a smooth increase in this difference, and a decrease in η, with the size of the halogen. The difference is magnified by a factor of 2 when considering $\angle$(XCX), and the quadrupole information defines an angle which is in all cases greater than the internuclear angle. Supporting evidence that this type of behavior is not limited to methylene halides comes from the data for CH_2BrCl [18] and CF_2BrCl [19], in which $\angle$(BrCCl) is consistent with the present pattern. This observation can be reformulated into a conjecture that angles defined by symmetry axes of the field gradient between nuclei with large electron density will exceed the internuclear angles. Of course, it is not entirely unexpected that the electron density at two terminal nuclei bound to a common atom would suffer some repulsive type distortion. Nevertheless, since we are measuring the properties of the field gradient and not the electron density itself we would not claim that these differences directly define the amount of "banana" character in covalent chemical bonds. The proper route forward would be to compare the experimental results with accurate *ab initio* electron density and field gradient calculations, although it is not certain that such small effects can yet be reliably modeled. We believe, however, that we have in this paper identified trends which, even though they are small, have an important bearing on the nature of the chemical bond.

Acknowledgments

One of the authors (Z.K.) appreciates many previous cooperations with Prof. A.C. Legon, Exeter, England, the experience from which contributed to rapid construction of the spectrometer. Financial support from the Institute of Physics, from the Committee for Scientific Research, project 2PO3B-044-08, and from the European Community, Contract CIPDT 92-5038 are acknowledged.

References

[1] W. Gordy, R.L. Cook, *Microwave Molecular Spectra*, Wiley, New York 1984.

[2] Y. Niide, H. Tanaka, I. Ohkoshi, *J. Mol. Spectrosc.* **139,** 11 (1990).

[3] Z. Kisiel, L. Pszczółkowski, W. Caminati, P.G. Favero, *J. Chem. Phys.* **105,** 1778 (1996).

[4] W.H. Flygare, W.D. Gwinn, *J. Chem. Phys.* **36,** 787 (1962).

[5] Z. Kisiel, P.W. Fowler, A.C. Legon, *J. Chem. Phys.* **93,** 3054 (1990).

[6] Z. Kisiel, L. Pszczółkowski, *J. Mol. Spectrosc.*, in press.

[7] T.J. Balle, W.H. Flygare, *Rev. Sci. Instrum.* **52,** 33 (1981).

[8] W.H. Press, B.P. Flannery, S.A. Teukolsky, W.T. Vetterling, *Numerical Recipes: The Art of Scientific Programming*, Cambridge University Press, Cambridge 1986.

[9] A.C. Legon, *Ann. Rev. Phys. Chem.* **34,** 275 (1983).

[10] C. Chuang, C.J. Hawley, T. Emilsson, H.S. Gutowsky, *Rev. Sci. Instrum.* **61,** 1629 (1990).

[11] Z. Kisiel, L. Pszczółkowski, to be published.

[12] J.K.G. Watson, in: *Vibrational Spectra and Structure*, Vol. 6, Ed. J. Durig, Elsevier, Amsterdam 1997, p. 1.

[13] H.M. Pickett, *J. Mol. Spectrosc.* **148,** 371 (1991).

[14] F. Tullini, G.D. Nivellini, M. Carlotti, B. Carli, *J. Mol. Spectrosc.* **138,** 355 (1989).

[15] J.L. Duncan, *J. Mol. Struct.* **158,** 169 (1987).

[16] *Landolt Börnstein Numerical Data and Functional Relationships in Science and Technology*, Ed. W. Martienssen, Springer Verlag, Berlin, Vol. II/6 (1974); Vol. II/19c (1992).

[17] R.W. Davis, M.C.L. Gerry, *J. Mol. Spectrosc.* **109,** 269 (1985).

[18] Y. Niide, I. Ohkoshi, *J. Mol. Spectrosc.* **136,** 17 (1989).

[19] Z. Kisiel, E. Białkowska-Jaworska, L. Pszczółkowski, *J. Mol. Spectrosc.*, in press.